ChemComm

Accepted Manuscript

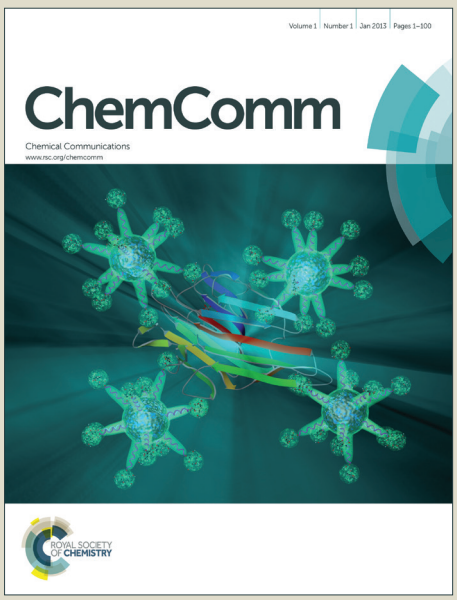

ROYAL SOCIETY OF CHEMISTRY

www.rsc.org/chemcomm

Cite this: DOI: 10.1039/coxx00000x

www.rsc.org/xxxxxx

ARTICLE TYPE

Ratiometric sensing of lysine through the formation of pyrene excimer: Experimental and computational studies

Sisir Lohar,[a] Damir A. Safin,[b] Archya Sengupta,[c] Ansuman Chattopadhyay,[c] Jesús Sanmartín Matalobos,[d] Maria G. Babashkina,*[b] Koen Robeyns,[b] Mariusz P. Mitoraj,*[e] Piotr Kubisiak,[e] Yann Garcia,[b] and Debasis Das*[a]

Received (in XXX, XXX) Xth XXXXXXXXX 20XX, Accepted Xth XXXXXXXXX 20XX
DOI: 10.1039/b000000x

Several pyrene based fluorescence probes undergo lysine assisted monomer to excimer conversion in a ratiometric manner. Intracellular lysine is detected under fluorescence microscope.

Lysine, an essential amino acid in the human body for the protein synthesis, undergoes catabolism in liver of mammals[1] *via* saccharopine pathway resulting in irreversible glutamate and α-aminoadipate formation, which subsequently faces deamination and oxidation. Lysine, a precursor for biosynthesis of carnitine, also plays an important role in β-oxidation of fatty acids.[2] High lysine concentration in plasma and urine indicates congenital metabolic disorders such as cystinuria or hyperlysinemia.[3] Thus, the trace level determination of lysine in biological systems is of great importance. Among available techniques such as HILIC column liquid chromatography,[4] liquid chromatography,[5] amperometric enzyme electrode[6] and fluorescence probes[7], the latter one being user friendly for biological studies. Despite existence of few lysine selective fluorescence probes,[8] its detection in biological medium is still challenging. Moreover, existing probes function at a single wavelength, susceptible to environmental parameters with a possibility of erroneous results for the quantitative determination. In contrast, ratiometric fluorescence sensing is more reliable.[9] The only reported pyrene based lysine sensor[10] suffers from number of the mentioned limitations. Pyrene exhibits a well-defined monomer emission at 370–430 nm along with an efficient excimer emission at about 480 nm.[11] The ratio of the excimer to monomer emission (I_E/I_M), being highly sensitive to the conformational change of the pyrene-appended receptors, is useful for the analytes sensing.[12] This inspired us to design several pyrene derivatives to engineer ratiometric lysine sensing *via* shifting of the monomer emission to the excimer form which will be useful for intracellular detection under a fluorescence microscope.

Two series of probes have been synthesized. The first series was obtained through the condensation of pyrene-1-carboxaldehyde with benzylamine (**BAPA**), picolylamine (**PAPA**), *n*-butylamine (**NBAPA**) and thiophene methyl amine (**PTA**) (Scheme S1 in ESI†).[13] The second series was synthesized by reacting benzylamine with anthracene-9-carboxaldehyde (**BAACA**) and naphthalene-1-carboxaldehyde (**BANA**) (Scheme S2 in ESI†). The crystal structures of **BAPA** and **BAACA** were elucidated by X-ray diffraction (Fig. S1–S4 and Tables S1 and S2 in ESI†). All compounds have been characterized by ESI-TOF mass spectrometry and ^{1}H NMR spectroscopy (Fig. S5–S10 in ESI†). **BAPA** exhibits a strong monomer emission at 400 nm along with a weak excimer emission at 505 nm, while addition of lysine induces a drastic change of its emission spectrum where the monomer emission is diminished significantly at the cost of excimer emission enhancement (Fig. 1) with a clear isoemissive point at 455 nm (Fig. S11 in ESI†).

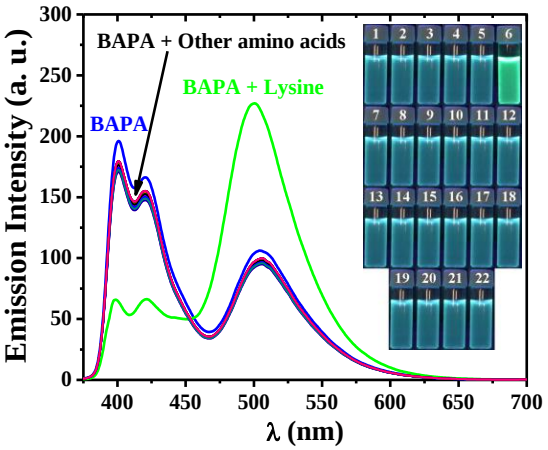

Fig. 1 Fluorescent spectra and UV light exposed colour of **BAPA** (10 μM) in the presence of different amino acids (50 μM) in HEPES buffered (0.1 M; MeOH:H_2O, 1:1 v/v; pH 7.4; λ_{exc} = 360 nm) solution (solution: blank (1), isoleucine (2), leucine (3), threonine (4), methionine (5), lysine (6), phenylalanine (7), tryptophan (8), valine (9), alanine (10), arginine (11), asparagines (12), aspartic acid (13), cysteine (14), glutamic acid (15), glutamine (16), glycine (17), ornithine (18), proline (19), serine (20), tyrosine (21) and cystine (22)).

Other amino acids show no changes of the monomer/excimer emission (Fig. 1). This might be due to the efficient H-bonding of the ε-amino group of lysine with imine N-centers of two **BAPA** molecules bringing two pyrene units closer to form the excimer (Fig. 2). Although arginine bears

View Article Online
DOI: 10.1039/C5CC01359C

also a free $-NH_2$ at the far end, an adjacent =NH group restricts the excimer formation. Interestingly, only MeOH and, less pronounced, EtOH favour the excimer formation (Fig. 3). It is known that in a dynamic excimer, emission arises from the pyrene dimer at the excited state whereas it occurs from the ground state in case of a static excimer.[11b] In **BAPA**, the excitation spectrum monitored at the monomer wavelength is almost identical to that of the excimer wavelength, indicating the latter emission from dynamic excimer (Fig. S12, left in ESI†).[11] On the other hand, the excitation spectrum of the [**BAPA**+lysine] adduct monitored at 505 nm is 20 nm red-shifted in comparison to that measured at 400 nm, indicating that the former emission originates from the static excimer (Fig. S12, right in ESI†).[11] Thus, chemical species responsible for the 505 nm and 400 nm emissions are different. The association constant of **BAPA** with lysine, derived using the Benesi-Hildebrand equation,[14] is 1100 M^{-1} (Fig. S13 in ESI†). **BAPA** offers the lowest detection limit for lysine, 5×10^{-8} M.

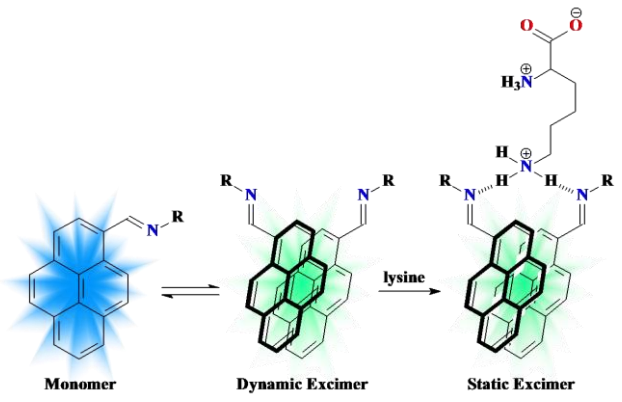

Fig. 2 Probable mechanism of the lysine sensing by **BAPA**, **PAPA**, **PTA** and **NBAPA**.

Upon gradual addition of lysine to **BAPA**, strong absorbance at 358 nm gradually decreases with concomitant increase of the band at 393 nm (Fig. S14 in ESI†) generating an isosbestic point at 367 nm. In the presence of lysine, the red-shift and band broadening of the UV spectrum of **BAPA** is attributed to the intermolecular π–π stacking of two pyrene units to form dimer in the ground state.[12b–e] This fact is also reflected in the ^{1}H NMR titration of **BAPA** by lysine (Fig. S15 in ESI†). Other amino acids do not interfere the [**BAPA**+lysine] adduct (Fig. S16 in ESI†). Additionally, the I_E/I_M ratio of free **BAPA** and its lysine adduct slightly increases under acidic condition. No appreciable lysine sensing is observed below pH 3. This might be due to the protonation of **BAPA** (Fig. S17 in ESI†). However, lysine sensing efficiency increases at higher pH, ranging from 3 to 8. Close to physiological pH 7.4, the I_E/I_M ratio reaches maximum, allowing to chose this pH for the entire studies.

Although **PAPA**, **PTA** and **NBAPA** show similar lysine selectivity (Fig. S18–S20 in ESI†), corresponding change in the I_E/I_M ratios of their lysine adducts are 3.8, 3.5 and 2.4 compared to 6.9 for **BAPA**. The association constants of **PAPA**, **PTA** and **NBAPA** with lysine are 800 $M^{-1/2}$, 1200 $M^{-1/2}$ and 2000 $M^{-1/2}$, respectively (Fig. S21–S23 in ESI†). Changes in the UV-Vis spectra are similar as for **BAPA** (Fig. S24–S26 in ESI†).

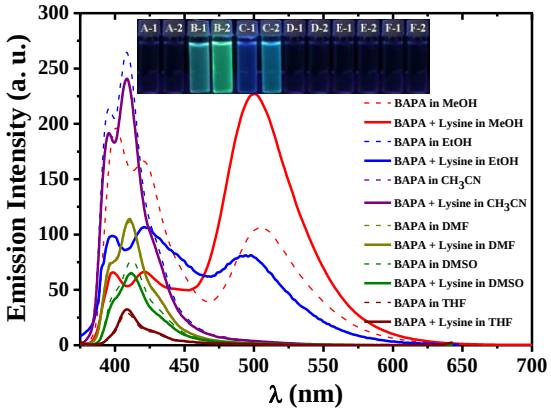

Fig. 3 Fluorescent spectra and UV light exposed color changes of **BAPA** (10 μM) in the absence and presence of lysine (50 μM) in different solvents (A = CH_3CN, B = MeOH, C = EtOH, D = DMF, E = DMSO and F = THF; 1 = **BAPA** and 2 = **BAPA** + lysine).

Lysine causes small fluorescence enhancement for **BAACA** and **BANA**. However no ratiometric sensing have been observed (Fig. S27 and S28 in ESI†). Moreover, fluorescence life time decay studies reveal that the presence of lysine enhances the life time of **BAPA** from 9 ns to 13 ns (Fig. S29 in ESI†).

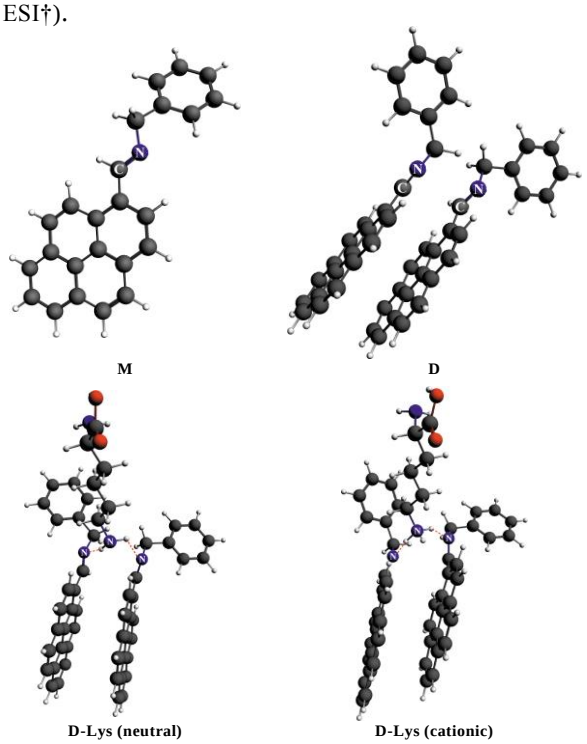

Fig. 4 DFT/BLYP-D3/TZ2P optimized structures of the monomer (**M**) and dimer (**D**) of **BAPA**, and the complex **D–Lys**. For **D–Lys** we have considered both the neutral and cationic lysine molecules. The hydrogen bonds of the type N···H–N in **D–Lys** are marked by dotted lines.

For deeper insight into the binding interaction between

View Article Online
DOI: 10.1039/C5CC01359C

BAPA and lysine, static DFT calculations, based on the ADF package[15] have been performed using the BLYP-D3/TZ2P protocol, which nicely describes non-covalent interactions (including the stacking ones).[16] Binding patterns between the **BAPA** units as well as between **BAPA** and lysine have been elucidated using ETS-NOCV[17] as implemented in the ADF program.[15] The lowest ground state energy structures were obtained for the monomer (**M**) and dimer (**D**) of **BAPA** as well as **BAPA**–lysine adducts (**D-Lys**) (Fig. 4).

The S_1 state of **M** was optimized using the Gaussian 09 program (revision D01).[18] The energy difference between S_1 and S_0 is 408 nm (Fig. S30 in ESI†) that nicely fits to the strong monomer emission band at 400 nm observed experimentally (Fig. 1).

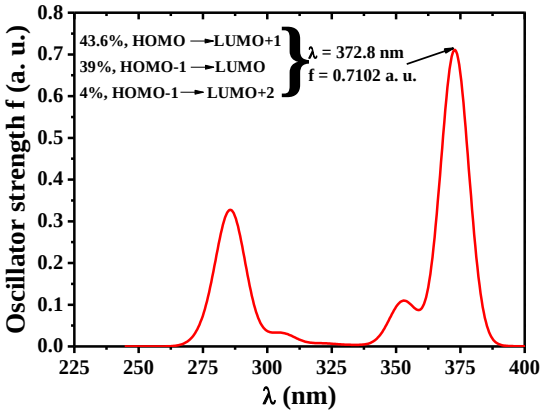

Fig. 5 Simulated TD-DFT/B3LYP/TZP spectrum of **D** in the gas phase (top) together with the contours of molecular orbitals (0.03 a. u.) involved in the dominant transitions (bottom).

Results of the ETS-NOCV calculations show that **D** is formed due to strong π–π stacking interactions. The calculated total interaction energy (ΔE_{total}) is –17.79 kcal/mol while the main stabilizing factor is the dispersion contribution ($\Delta E_{dispersion}$) –29.57 kcal/mol followed by significantly less important parameters like electrostatic (ΔE_{elstat}) –9.50 kcal/mol and the orbital interaction (ΔE_{orb}) –4.46 kcal/mol (Table S3 in ESI†). Such a significant dimerization energy suggests that **BAPA** units in solution can indeed aggregate *via* stacking interactions. We have further considered the binding of neutral and cationic forms of lysine with **D** (Fig. 4). The binding of cationic lysine is predominantly studied as this form exists at physiological pH ~7. It was found that the neutral lysine is rather weakly bonded to **D** with the interaction energy being –9.41 kcal/mol and the electrostatic stabilization is a dominant factor (Table S3 in ESI†). It should be noted that this binding pattern involves single hydrogen bonding bridge of the type N···H–N between **D** and lysine (Fig. S31 in ESI†). More importantly, ETS-NOCV studies indicate that, considering the binding of the cationic lysine with **D**, the stabilization becomes very high with the interaction energy being –63.65 kcal/mol (Table S3 in ESI†). Interestingly, in this case, not the electrostatic (ΔE_{elstat} = –51.62 kcal/mol), but the orbital (ΔE_{orb} = –56.04 kcal/mol) interaction term appears to be the leading stabilizing term (Table S3 in ESI†).

The NOCV deformation density contributions ($\Delta\rho_1$, $\Delta\rho_2$, $\Delta\rho_3$, $\Delta\rho_4$), along with the corresponding orbital interaction terms ($\Delta E_{orb}(1)$, $\Delta E_{orb}(2)$, $\Delta E_{orb}(3)$, $\Delta E_{orb}(4)$) are shown in Fig. S32 in ESI†. Two major terms ($\Delta\rho_1$ and $\Delta\rho_2$) with corresponding $\Delta E_{orb}(1)$ = –18.26 kcal/mol and $\Delta E_{orb}(1)$ = –9.73 kcal/mol, characterize the formation of two hydrogen bonding bridges of the type N···H–N, which connect the NH_3^+ fragment of lysine with two stacking layers of **BAPA**. They originate from the charge donation from the lone pair of nitrogen centers to the empty σ*(N–H) of lysine. The third and the fourth terms ($\Delta\rho_3$ and $\Delta\rho_4$), corresponding to the stabilizations $\Delta E_{orb}(3)$ = –3.17 kcal/mol and $\Delta E_{orb}(4)$ = –2.97 kcal/mol, respectively, exhibit the interaction of NH_3^+ of lysine with both the *o*-phenyl C_{ortho}–H bonds and the CH=N fragment of the **BAPA** unit.

Calculation of the ^{1}H NMR proton shifts upon interaction of lysine with **D**, using the GIAO approach as implemented in the ADF program,[15] reveals the qualitative agreement with experiment (Fig. S15 in ESI†). The *o*-phenyl and CH=N protons, engaged in the interaction with **D**, are high-field shifted by 0.715 and 0.24 ppm, respectively. Moreover, it is also consistent with the presence of weak C_{ortho}–H···H_3N^+ and CH=N···H_3N^+ interactions, identified by $\Delta\rho_3$ and $\Delta\rho_4$.

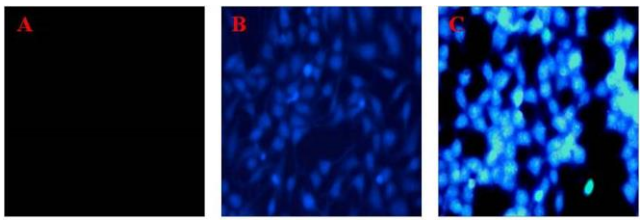

Fig. 6 Fluorescence microscope images of the MCF7 cells after incubation for 2 h with lysine (50 μM) (**A**), followed by addition of **BAPA** (20 μM) (**B**). Cells after incubation for 2 h with **BAPA** (20 μM) followed by addition of lysine (50 μM) (C).

In order to gain further insight into the changes of the absorption spectra of **BAPA** upon interaction with lysine, TD-DFT calculations have been performed using the ADF program[15] for **D** and **D-Lys (cationic)**. The simulated spectrum for the gas phase structure of **D** indicates that the dominant absorption band, having an oscillator strength f = 0.7102 a.u., is observed at 372.8 nm. Decomposition of this transition into the molecular orbitals shows that the absorption is of the π→π* type and it engages both stacked **BAPA** rings (Fig. 5). More importantly, complexation of **D** with lysine leads to both decrease in the oscillator strength from f = 0.7102 a. u. to f = 0.6534 a. u. as well as to the red-shift of the dominant π→π* band from 372.8 nm to 402.5 nm (Fig. S33 in ESI†). These observations are qualitatively in line with the experimental spectra (Fig. S14 in ESI†). It is interesting to note that the TD-DFT absorption spectra for **D-Lys (neutral)**

have similar characteristics of the dominant band when compared with **D** (Fig. S34 in ESI†).

BAPA was used to image lysine in human breast cancer cells, MCF7, under fluorescence microscope. **BAPA** can stain lysine in living cells without any harm, making it useful to monitor lysine accumulation in biological systems (Fig. 6).

S. Lohar thanks CSIR for fellowship. Help from CAS (UGC) is gratefully acknowledged.

Notes and references

[a]*Department of Chemistry, The University of Burdwan, 713104, Burdwan, West Bengal, India. Fax: (+91) 342 2530452; Tel: (+91) 342 2533913; E-mail: ddas100in@yahoo.com*

[b]*Institute of Condensed Matter and Nanosciences, Molecules, Solids and Reactivity (IMCN/MOST), Université Catholique de Louvain, Place L. Pasteur 1, 1348 Louvain-la-Neuve, Belgium. Fax: +32(0) 1047 2330; Tel: +32(0) 1047 2831; E-mail: maria.babashkina@gmail.com*

[c]*Department of Zoology, Visva Bharati University, Santiniketan, West Bengal, India.*

[d]*Departamento de Química Inorgánica, Facultade de Química, Avda. Das Ciencias s/n, 15782, Santiago de Compostela, Spain.*

[e]*Department of Theoretical Chemistry, Faculty of Chemistry, Jagiellonian University, R. Ingardena 3, 30-060 Cracow, Poland. E-mail: mitoraj@chemia.uj.edu.pl*

† Electronic Supplementary Information (ESI) available: Additional data, Schemes S1 and S2, Fig. S1–S34 and Tables S1–S3. CCDC numbers 931269 (**BAPA**) and 938292 (**BAACA**). For ESI and crystallographic data in CIF or other electronic format see DOI: 10.1039/b000000x

1 K. Higashino, M. Fujioka and Y. Yamamura, *Arch. Biochem Biophys.*, 1971, **142**, 606.

2 V. Tanphaichitr and H. P. Broquist, *J. Biol. Chem.*, 1973, **248**, 2176.

3 (*a*) P. Felig, *Annu. Rev. Biochem*., 1975, **44**, 933; (*b*) C. Hirayama, K. Suyama, Y. Horie, K. Tanimoto and S. Kato, *Biochem. Med. Metab. Biol.*, 1987, **38**, 127.

4 P. Bhandare, P. Madhavan, B. M. Rao and N. Someswarrao., *J. Chem. Pharm. Res.*, 2010, **2**, 580.

5 A. Hernández, M. A. Serrano, M. M. Muñoz and G. Castillo, *J. Chromatogr. Sci.*, 2001, **39**, 39.

6 M. G. Lavgnini, D. Moscone, D. Campagnone, C. Crimisini and G. Palleschi, *Talanta*, 1993, **40**, 1301.

7 M. Wehner, T. Schrader, P. Finocchiaro, S. Failla and G. Consiglio, *Org. Lett*., 2000, **2**, 605.

8 (*a*) M. Wehner, T. Schrader, P. Finocchiaro, S. Failla and G. Consiglio, *Org. Lett*., 2000, **2**, 605; (*b*) S. Sasaki, A. Hashizume, D. Citterio, E. Fujii, K. Suzuki, *Tetrahedron Lett*., 2002, **43**, 7243; (*c*) K. Secor, J. Plante, C. Avetta and T. Glass, *J. Mater. Chem*., 2005, **15**, 4073; *d*) C. P. Mandl and B. Konig, *J. Org. Chem*., 2005, **70**, 670.

9 (*a*) L.-Y. Niu, Y.-S. Guan, Y.-Z. Chen, L.-Z. Wu, C.-H. Tung, Q.-Z. Yang, *J. Am. Chem. Soc.*, 2012, **134**, 18928; (*b*) R. Gui, X. An, H. Sua, W. Shen, L. Zhu, X. Ma, Z. Chen and X. Wang, *Talanta*, 2012, **94**, ***295***; (*c*) P. Das, A. K. Mandal, N. B. Chandar, M. Baidya, H. B. Bhatt, B. Ganguly, S. K. Ghosh and A. Das, *Chem. Eur. J*. 2012, **18**, 15382.

10 Y. Zhou, J. Won, J. Y. Lee and J. Yoon, *Chem. Commun*., 2011, **47**, 1997.

11 (*a*) F. M. Winnik, *Chem. Rev*., 1993, **93**, 587; (*b*) M.-H. Yang, P. Thirupathi and K.-H. Lee, *Org. Lett*., 2011, **13**, 5028.

12 (*a*) C. Broan, *Chem. Commun*., 1996, 699; (*b*) F. D. Lewis, Y. Zhang and R. L. Letsinger, *J. Am. Chem. Soc.*, 1997, **119**, 5451; (*c*) J. Lou, T. A. Hatton and P. E. Laibinis, *Anal. Chem.*, 1997, **69**, 1262; (*d*) A. T. Reis e Sousa, E. M. S. Castanheira, A. Fedorov, J. M. G. Martinho, *J. Phys. Chem. A*, 1998, **102**, 6406; (*e*) Y. Suzuki, T. Morozumi, H. Nakamura, M. Shimomura, T. Hayashita and R. A. Bartsch, *J. Phys. Chem. B*, 1998, **102**, 7910.

13 A. Banerjee, A. Sahana, S. Das, S. Lohar, B. Sarkar, S. K. Mukhopadhyay, J. S. Matalobos and D. Das., *Dalton Trans.*, 2013, **42**, 16387.

14 H. A. Benesi and J. H. Hildebrand, *J. Am. Chem. Soc.*, 1949, **71**, 2703.

15 (*a*) G. te Velde, F. M. Bickelhaupt, E. J. Baerends, C. Fonseca Guerra, S. J. A. van Gisbergen, J. G. Snijders and T. Ziegler, *J. Comput. Chem.*, 2001, **22**, 931 and references therein; (*b*) E. J. Baerends, J. Autschbach, D. Bashford, A. Bérces, F. M. Bickelhaupt, C. Bo, P. M. Boerrigter, L. Cavallo, D. P. Chong, L. Deng, R. M. Dickson, D. E. Ellis, M. van Faassen, L. Fan, T. H. Fischer, C. Fonseca Guerra, A. Ghysels, A. Giammona, S. J. A. van Gisbergen, A. W. Götz, J. A. Groeneveld, O. V. Gritsenko, M. Grüning, F. E. Harris, P. van den Hoek, C. R. Jacob, H. Jacobsen, L. Jensen, G. van Kessel, F. Kootstra, M. V. Krykunov, E. van Lenthe, D. A. McCormack, A. Michalak, M. Mitoraj, J. Neugebauer, V. P. Nicu, L. Noodleman, V. P. Osinga, S. Patchkovskii, P. H. T. Philipsen, D. Post, C. C. Pye, W. Ravenek, J. I. Rodríguez, P. Ros, P. R. T. Schipper, G. Schreckenbach, M. Seth, J. G. Snijders, M. Solà, M. Swart, D. Swerhone, G. te Velde, P. Vernooijs, L. Versluis, L. Visscher, O. Visser, F. Wang, T. A. Wesolowski, E. M. van Wezenbeek, G. Wiesenekker, S. K. Wolff, T. K. Woo, A. L. Yakovlev and T. Ziegler, Theoretical Chemistry, Vrije Universiteit: Amsterdam.

16 W. Gao, H. Feng, X. Xuan and L. Chen, *J. Mol. Model.*, 2012, **18**, 4577.

17 (*a*) M. Mitoraj, A. Michalak and T. Ziegler, *J. Chem. Theory Comput.*, 2009, **5**, 962; (*b*) M. Mitoraj and A. Michalak, *J. Mol. Model.*, 2007, **13**, 347.

18 Gaussian 09, Revision D.01, M. J. Frisch, G. W. Trucks, H. B. Schlegel, G. E. Scuseria, M. A. Robb, J. R. Cheeseman, G. Scalmani, V. Barone, B. Mennucci, G. A. Petersson, H. Nakatsuji, M. Caricato, X. Li, H. P. Hratchian, A. F. Izmaylov, J. Bloino, G. Zheng, J. L. Sonnenberg, M. Hada, M. Ehara, K. Toyota, R. Fukuda, J. Hasegawa, M. Ishida, T. Nakajima, Y. Honda, O. Kitao, H. Nakai, T. Vreven, J. A. Montgomery, Jr., J. E. Peralta, F. Ogliaro, M. Bearpark, J. J. Heyd, E. Brothers, K. N. Kudin, V. N. Staroverov, R. Kobayashi, J. Normand, K. Raghavachari, A. Rendell, J. C. Burant, S. S. Iyengar, J. Tomasi, M. Cossi, N. Rega, J. M. Millam, M. Klene, J. E. Knox, J. B. Cross, V. Bakken, C. Adamo, J. Jaramillo, R. Gomperts, R. E. Stratmann, O. Yazyev, A. J. Austin, R. Cammi, C. Pomelli, J. W. Ochterski, R. L. Martin, K. Morokuma, V. G. Zakrzewski, G. A. Voth, P. Salvador, J. J. Dannenberg, S. Dapprich, A. D. Daniels, Ö. Farkas, J. B. Foresman, J. V. Ortiz, J. Cioslowski, and D. J. Fox, Gaussian, Inc., Wallingford CT, 2009.

